Journal of Cleaner Production 330 (2022) 129789

Contents lists available at ScienceDirect

Journal of Cleaner Production

journal homepage: www.elsevier.com/locate/jclepro

Short-time acoustic and hydrodynamic cavitation improves dispersibility and functionality of pectin-rich biopolymers from citrus waste.

Jin Chu [a], Philip Metcalfe [b], Holly V. Linford [c], Siying Zhao [a], Francisco M. Goycoolea [a], Shiguo Chen [d], Xingqian Ye [d], Melvin Holmes [a], Caroline Orfila [a,*]

[a] School of Food Science and Nutrition, University of Leeds, Leeds, UK
[b] Biopower Technologies Limited, Wolverton Mill, UK
[c] School of Physics and Astronomy, University of Leeds, Leeds, UK
[d] College of Biosystems Engineering and Food Science, Zhejiang Key Laboratory for Agro-Food Processing, Fuli Institute of Food Science, Zhejiang University, Hangzhou, China

ARTICLE INFO

Handling Editor: Prof. Jiri Jaromir Klemeš

Keywords:
Citrus pectin
Hydrodynamic cavitation
Acoustic cavitation
Dispersion
Gel
Waste

ABSTRACT

Pectin is a valuable biopolymer used as a natural, clean label additive for thickening and gelling. However, industry faces issues with dispersibility and stability of pectin formulations. To address these issues, the effect of short processing time (30–180 s) with hydrodynamic (HC) and acoustic cavitation (AC) on the dispersibility and gelling functionality of mandarin pectin-rich polysaccharide (M-PRP) was investigated. Short-time processing with HC and AC did not affect polymer composition. HC, but not AC, decreased polydispersity index (PDI) from 0.78 to 0.68 compared to the control. Electron and atomic force microscopy showed that HC and AC decreased aggregation of fibrous and matrix polymers. Both treatments increased apparent viscosity significantly from 0.059 Pa s to 0.30 Pa s at 10 $^{-s}$. The pectin dispersions showed good gelling capacity upon addition of calcium (final conc. 35 mM). HC and AC treatments for 150 s led to gels that were 7 and 4 times stronger (as measured by peak force) than the control with more homogeneous, less porous structures. In conclusion, short-time HC and AC can improve the dispersibility and functionality of citrus pectin without affecting composition, and are promising technologies to facilitate the use of pectin in industry applications.

1. Introduction

Citrus fruits are the most consumed fruits in the world with production estimated at 124,000 tons per year in 2016 (FAO, 2016). Around 40–50% is processed by the global agro-food industry, generating over 50,000 tons of by-products including solid (peels, albedo and seeds) and liquid (washing and canning water) streams (Sharma et al., 2017). These represent a potentially valuable biological resource for extraction of functional biopolymers and small molecules (Yan et al., 2018; Sharma et al., 2017; Zema et al., 2018). China produced around 32,000 tons of citrus of which 60% are mandarins (*Citrus reticulata*). These are largely processed by canning in a sequence that includes peeling, segment separation, segment membrane removal, washing, syrup addition and in-can thermal processing (Chen et al., 2017). The segment removal and washing steps generate around 60,000 m^3 of liquid waste per day (Chen et al., 2017). The segment membrane is removed chemically by solubilisation of its polymers through serial acid and alkaline treatments. The waste stream of this process is a viscous liquid rich in pectic polysaccharides which is precipitated with ethanol and dried to produce a food-grade powdered ingredient at a commercial scale (Chen et al., 2017). Mandarin membrane alcohol insoluble solids (AIS) have been shown to be composed of 80% polysaccharides, with a high proportion (around 60% w/w) of pectins (Coll-Almela et al., 2015). The polysaccharides recovered industrially from mandarin waste water were shown to have a similar composition (Zhang et al., 2018a) and comparable properties to the polysaccharides recovered from a lemon waste stream (Dimopoulou et al., 2019).

Pectin is a complex heterogeneous polysaccharide, containing structural domains including homogalacturonan (HG), rhamnogalacturonan I (RGI) and rhamnogalacturonan II (RGII). Its chemical composition and structure varies between different fruits, parts within the fruit and growth stages (Voragen et al., 2009, Voragen et al., 1995). For example, lemon membrane residues contained more branched RGI than the neighbouring albedo tissue (Dimopoulou et al., 2019). Pectin is usually classified as high methoxy or low methoxy according to the

* Corresponding author.
E-mail address: c.orfila@leeds.ac.uk (C. Orfila).

https://doi.org/10.1016/j.jclepro.2021.129789
Received 24 June 2021; Received in revised form 19 November 2021; Accepted 20 November 2021
Available online 26 November 2021

Abbreviations

AFM	Atomic Force Microscopy
AC	Acoustic cavitation
DM	Degree of methylation
ELISA	Enzyme-linked immunosorbent assay
HC	Hydrodynamic cavitation
HG	Homogalacturonan
M-PRP	Mandarin pectin-rich polysaccharides
PDI	Polydispersity index
RGI	Rhamnogalacturonan I
RGII	Rhamnogalacturonan II
SEM	Scanning Electron Microscopy

degree of methyl esterification (DM), which influences pectin properties especially its solubility and gel-forming characteristics (Morris et al., 2000). Alkaline treatment results in pectin de-esterification which decreases its water solubility (Voragen et al., 1995), but increases its ability to form strong visco-elastic gels in the presence of calcium through HG-calcium cross links (Willats et al., 2001). Pectin recovered from citrus peels and membranes has been shown to have relatively high RGI content with high degree of branching (Zhang et al., 2018b; Cui et al., 2019; Dimopoulou et al., 2019) compared to other fruit such as berries (Taboada et al., 2010). Evidence of the importance of neutral side chains in modulating pectin rheological properties is emerging. It has been suggested that arabinan side chains may strengthen gels by stabilising HG-calcium junction zones (Zheng et al., 2020). RGI side chains improve emulsifying properties depending on the chain length, with medium length chains being optimal for emulsion formation and stability (Alba and Kontogiorgos, 2017; Kpodo et al., 2018). Physical, chemical and enzymatic methods of extraction and post-extraction treatments may influence pectin composition and functionality (Mao et al., 2019). For example, canning can increase the solubility of the cell wall polysaccharides particularly those rich in neutral sugars (Chu et al., 2020) while disruption of cell wall structure by high shear homogenisation led to 10% increase in the solubility of the polysaccharides from fruit tissue (Chu et al., 2017).

Pectin is a valuable biopolymer for the food industry, used as a natural, clean label additive for thickening and gelling (INGREDION, 2014; Varela and Fiszman, 2013; Chan et al., 2017). The global market for pectin was estimated at 400 million euros in 2014 (Mamma et al., 2014). However, the industry faces issues with dispersibility and stability of pectin formulations. Dispersion methods can influence rheological properties and stability of pectin gels (Muñoz-Labrador et al., 2018). Long dispersion times increases the risk of microbial contamination, while insufficient dispersion leads to phase separation and precipitation. Fibre hydration may also influence its prebiotic properties (Williams et al., 2019).

When a liquid undergoes a reduction in the applied environmental pressure which is below its vapour pressure, vapour-filled bubbles or cavities can form within the bulk of the liquid. On re-application of a higher applied pressure, these cavities will implode and, in doing so will generate localised shock waves which generate turbulent (non-laminar) flow and cause significant disruption to neighbouring surfaces, particles or fibres. This phenomenon is known as cavitation and can be created through pressure displacements generated through mechanical i.e. hydrodynamic cavitation (HC) or acoustic methods. In the case of acoustic cavitation (AC), also known as ultrasound cavitation, the change in pressure is generated by high frequency (>20 kHz) sonic waves, while in hydrodynamic cavitation (HC), changes in pressure are generated by mechanical waves. In both cases, successive compression cycles generate pressure differences that lead to repetitive bubble formation and collapse generating localised turbulent fluid flow as well as high temperature 'hot-spots'. The cavitation intensity depends on a number of factors including the power and amplitude of the pressure waves, and the properties of the bulk fluid. Wave propagation, bubble formation and stability are a function of solvent and solute properties e.g. viscosity, surface tension and particle volume fraction. In addition to the physical disruption and abrasion of particles, reactive species can also cause chemical modifications of macromolecules. It can be difficult to differentiate between the cavitation, shear, thermal and chemical effects (Ghorbani et al., 2019).

AC has been used extensively in industrial applications to extract, emulsify, sterilize and increase the rate of biochemical reactions (Ashokkumar, 2015), including extracting and modifying pectin. For instance, intensity AC (12.56 W/cm^2, 27.95 min, 66.7 °C) was used to efficiently extract pectin from grapefruit peels (Wang et al., 2015). By varying the intensity, time and temperature (up to 544 W/cm^2, up to 30 min, up to 40 °C), the structure of pectin could be modified (Zhang et al., 2013; Wang et al., 2018). AC treatments (20 kHz, 0–540 W mL^{-1}, 5–30 min) tend to de-esterify and depolymerize pectin molecules, while longer (>30 min) high intensity AC treatments caused biopolymer cross-linking leading to increase in particle size and aggregation of particles (Zhang et al., 2013). AC processing (18–27 W mL^{-1}, 20 °C, 5–30 min) was used as a pre-treatment to enzymatic modification of citrus pectin (Ma et al., 2018). Low intensity AC treatments for 90 min at 30 °C increases solubility of antioxidant compounds but can result in cloud formation in fruit drinks, suggested to be the result of protein denaturation and aggregation (Sattar et al., 2019).

HC has also been used in industrial applications for sterilisation and waste water treatment (Save et al., 1997; Sivakumar and Pandit, 2002; Gogate, 2011). The theory behind HC and its application in waste treatment has been clearly explained by Sun et al. (2020). HC can also be used in microliter scale, for example in the generation of radical-induced fluorescence in microfluidic devices (Perrin et al., 2021). A range of HC set ups have been used to differentially inactivate microorganisms (Zupanc et al., 2019). In food applications, HC has been used at the end of fermentation processes (Albanese et al., 2015) including in industrial-scale beer brewing (Albanese et al., 2017), and to sterilize liquid food at pilot scale (Milly et al., 2007, 2008). HC has been suggested to be an alternative to AC in food processing applications involving large volumes (Ashokkumar et al., 2011). Studies have also applied HC for the purpose of extraction of pectin and bioactive compounds (Meneguzzo et al., 2019; Katariya et al., 2020). Meneguzzo et al. (2019) extracted low DM pectin, polyphenols and terpenes from orange peel at kg scale using a circular Venturi-shaped reactor, with processing times >120 min without temperature control. Katariya et al. (2020) used HC for relatively shorter processing time (5–25 min) as a pasteurisation process for orange juice. The process preserved the bioactive content and inactivated enzymes such as pectin methyl esterase and peroxidase. However, use of short-time HC for pectin dispersions (or other biopolymers) has not been previously investigated.

Most of the studies have focused on long (>30 min) processing times with AC or HC. The aim of this study was to compare the effect of very short time (up to 180 s) AC and HC processing, with similar energy densities, on the dispersibility and gelling functionality of mandarin pectin rich polysaccharides recovered from canning waste, referred to here as M-PRP. The results of this study provide preliminary evidence that very short time cavitation processing times may benefit the stability and functionality of pectin in food and non-food applications.

2. Material and methods

2.1. Pectin dispersion

Mandarin pectin-rich polysaccharides (M-PRP) were recovered from industrial mandarin canning water, produced by Huayu Co. Ltd (China), according to the scheme in Fig. S1 and as described in detail in Chen et al. (2017).

M-PRP was re-suspended in de-ionized water (1% w/v) using three methods: conventional stirring, acoustic cavitation (AC) and hydrodynamic cavitation (HC). For conventional stirring, the pectin suspension was continuously stirred using a lab magnetic stirrer overnight (12 h) at room temperature. For AC, pectin suspensions were treated with a high-intensity ultrasound processor, model Q125 (Qsonica LLC, USA) fitted with a 3.0 mm diameter titanium probe. The settings were power 125 W, frequency of 20 kHz, amplitude 80% pulse duration of on-time 1 s and off-time 2 s for 30, 60, 90, 120, 150, and 180 s. For HC, pectin suspensions were treated in a hydrodynamic rotational cavitation processor (model 2.2, Biopower Technologies, UK). The settings were cavitation number 0.26, inlet pressure of 7 Bar, flow rate 20 L/min for 30, 60, 90, 120, 150, and 180 s. The system uses a 2.2 KW pump. The experimental set ups are presented in Fig. 1 with details of the HC streams in Table 1.

Table 1
HC streams.

Stream	Start	End
1	Holding Tank (T101)	Valve (V101)
2	Valve (V101)	Pump (P101)
3	Pump (P101)	Cavitator (C101)
4	Cavitator (C101)	Holding Tank (T101)

Energy density was calculated according to equation (1).

$$\text{Energy Density } [\text{J L}^{-1}] = \frac{\text{Power[W]} \times \text{Time[s]}}{\text{Volume[L]}} \quad (1)$$

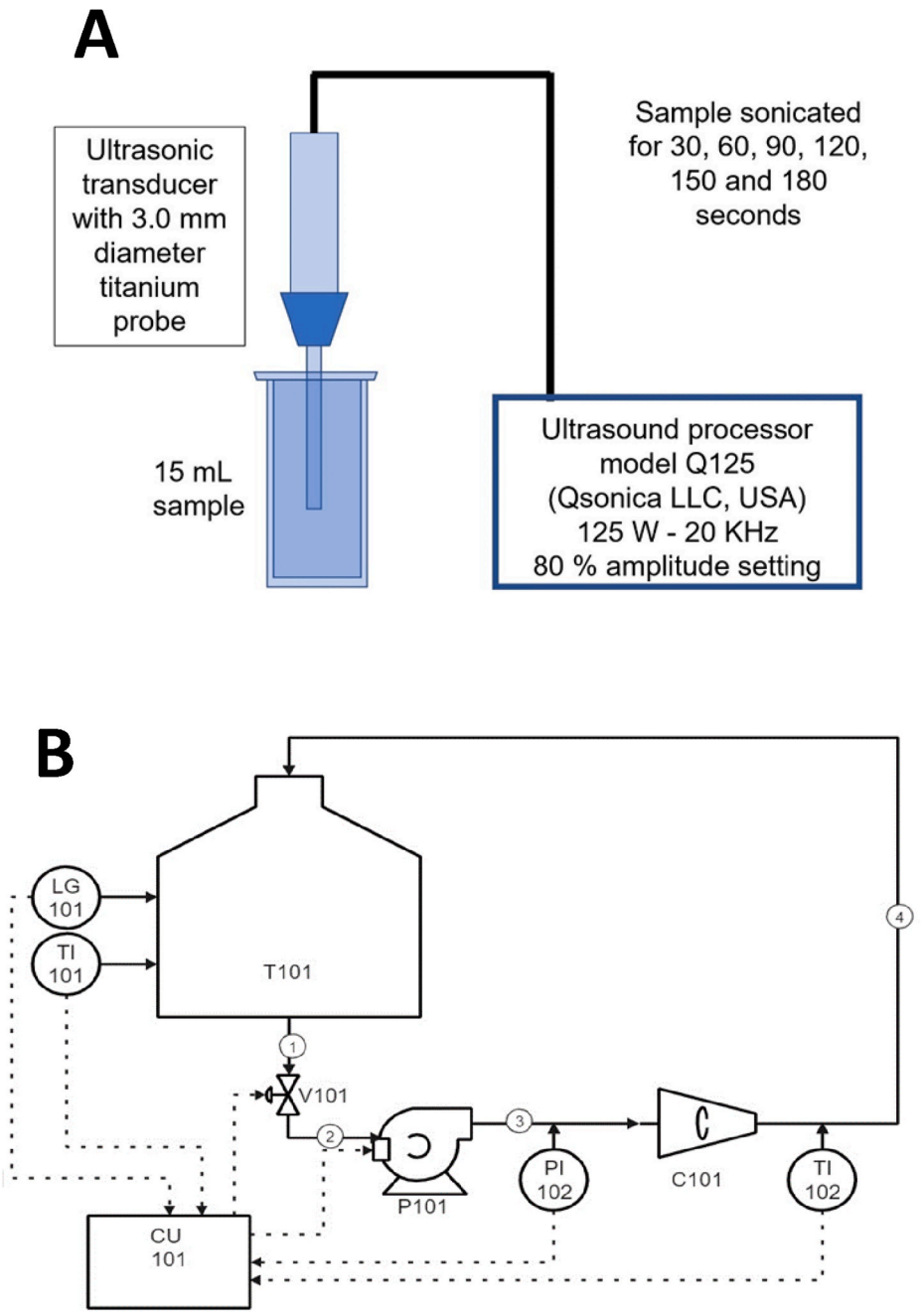

Fig. 1. Diagrams of experimental set up for A) acoustic cavitation (AC) and B) hydrodynamic cavitation (HC). For HC, C101 = rotational cavitator; CU101 = control unit, LG101 = level gauge, P101 = centrifugal pump; PI101 = pressure indicator; T101 = holding tank = TI101 = Temperature Indicator – Tank; TI102 = Temperature Indicator – Cavitator; V101 = Control valve.

2.2. Particle size measurement

Particle size distribution and polydispersity was determined using a Mastersizer 3000 (Malvern Panalytical Ltd, Malvern, UK) at room temperature. Following dispersing treatments, samples (1% w/v pectin solution) were diluted in deionised water at 2000 rpm until an obscuration around 5% was obtained. The background and sample integration times were 20 and 10 s, respectively. Size distribution was calculated as weight-average sizes, expressed as $D_{3,2}$ and $D_{4,3}$. The experiments were repeated at least three times.

2.3. Rheology

The viscosity of the suspensions were measured using a Kinexus rheometer (Malvern Instruments Ltd, Worcestershire, UK) equipped with a 60 mm diameter cone and plate geometry. Temperature was fixed (25 °C) and an adiabatic hood was placed to avoid evaporation during the experiments. The shear viscosity was obtained for shear rates ranging from 0.1 to 100.0 s^{-1}. For each point, the measured stress stability was ensured within a 0.5% of variability. The rheological properties of consistency index K (Pa s^n), flow behaviour index n were fitted to measured data of shear stress σ (Pa) and viscosity μ (Pa s) as functions of shear rate $\dot{\gamma}$ (s^{-1}) using equation (2). The experiments were repeated at least three times.

$$\mu = K\dot{\gamma}^{n-1} \tag{2}$$

The consistency K provides a measure of the apparent viscosity (typically at a shear rate of 1 s^{-1}. The flow index indicates the nature of the fluid with Newtonian fluids $n = 1$, $n < 1$ for shear thinning and $n > 1$ for shear thickening. Typical oral shear rates were estimated at 10 s^{-1} (Rabiti et al., 2018).

2.4. Composition analysis

Uronic acid was measured using a method was adapted from Cesaretti et al. (2003) with minor changes. Briefly, 50 μl of sample was added into a 15 ml acid and heat resistant tube. Then 200 ml of freshly prepared 25 mM sodium tetraborate in sulfuric acid was added. The tubes were heated at 100 °C for 10 min in a heating block. After cooling at room temperature for 15 min, 50 ml of 0.125% carbazole in absolute ethanol were carefully added. Tubes were heated again at 100 °C for 10 min and cooling at room temperature for 15 min. Samples (200 μl) were then transferred to a microplate and the absorbance read in a microplate reader at a wavelength of 550 nm. The experiments were repeated at least three times.

The nitrogen content was measured using inductively coupled plasma mass spectrometry at RIAIDT-USC (Santiago de Compostela, Spain) analytical facilities. The protein content was estimated by multiplying the determined nitrogen content by a nitrogen-to-protein conversion factor 6.25. Ash content was determined by dry-ashing; 1 g of samples were heated at 500 °C furnace for 12 h, then cooled in a desiccator. The weight difference before and after burning was recorded as the ash content. The experiments were repeated at least three times.

2.5. Polysaccharide composition

An ELISA based technique which allows rapid analysis of polysaccharide epitopes was used (Pattathil et al., 2010; Rongkaumpan et al., 2019). Pectin suspensions were adjusted to 0.05 μg/ml in 50 mM sodium carbonate (pH 9.6) and 200 μl used to coat immunosorbent plates (Nunc Immuno Plate F96 MaxiSorp) overnight at 4 °C. Plates were washed extensively with de-ionized water (10 times), then non-specific sites blocked with 5% (w/v) non-fat milk powder in phosphate buffer saline (MP-PBS, 200 μl/well) for 2 h at room temperature. Following a wash with de-ionized water (10 times), plates were incubated with primary antibody diluted 1:10 in MP-PBS (100 μl/well) and incubated for 1.5 h at RT. Then the plates were washed with de-ionized water (10 times), and incubated with secondary antibody in MP-PBS (100 μl/well) for 1.5 h at room temperature. Secondary antibodies were anti-rat IgG conjugated with horse radish peroxidase obtained from Invitrogen (Merck A9037-1 ML). The plates were washed with de-ionized water (10 times), followed by the addition of the 150 μl/well HRP substrate to generate the signal. The substrate contained 1 M sodium acetate buffer pH 6.0, tetramethylbenzidine, 6% (v/v) hydrogen peroxide and distilled water with a ratio of 100:10:1:1000. The reaction was stopped by adding 2 N sulfuric acid and the absorbance was determined at 450 nm using a plate reader (Multiskan Fc microplate readers, Finland). Thirty-two primary antibodies directed to glycans were used in the analysis, with 5 replicates each.

2.6. Scanning Electron Microscopy (SEM)

Pectin suspensions were diluted in distilled water to 10 μg ml^{-1}, placed on a copper plate and dried at low temperature (50 °C) in a convection oven. Gel samples were sectioned transversally and freeze-dried onto the plates. Samples were coated with a thin layer of iridium (4 nm) using a sputter coater (Cressington 208HR). Samples were then imaged using an FEI Nova NanoSEM 450 FEG-SEM operating at 3 kV. Representative images were selected for each sample.

2.7. Atomic force microscopy (AFM)

Pectin suspensions were diluted in distilled water to 10 μg ml^{-1}, placed on a glass slide and dried at low temperature (50 °C) in a convection oven. Dried samples were imaged using a Bruker Dimension FastScan AFM in PF QNM mode (Peak Force Quantitative Nanomechanical Mapping). A silicon nitride cantilever (ScanAsyst-Air, Bruker) with a nominal spring constant of 0.4 N m^{-1} was used for scanning. At least 10 regions per sample were randomly selected for imaging, with images showing separate (i.e. individually distinguishable) pectin fibrils used for further analysis. All images are at least 512 × 512 pixels. Representative images were selected for each sample.

Images were analysed using NanoScope Analysis software (v1.90). Images were flattened to remove bow from each scan line. Pectin fibril diameter was measured using the section tool, with fibrils selected manually. Fibril diameter was corrected for tip broadening effects using the method from (Morris et al., 1997) with tip radius given by the maximum value from the manufacturer (12 nm). The mean corrected diameter for 100 fibrils each for stirred, ultrasound and cavitation samples is given.

2.8. Calcium-pectin gel formation and characterisation

Calcium-pectin gels were prepared as described previously (Willats et al., 2001). 900 μl of pectin solution (1% w/v) was transferred to a 2 ml syringe from which the nozzle end been removed (inner diameter 0.9 cm). On top of the pectin solution, 67 μl of 500 mM $CaCl_2$ was added (final concentration 35 mM). The syringes were sealed and equilibrated at 4 °C for 24–48 h. The gel was removed using the syringe plunger and the gel cut to 1 cm height using a sharp mould. A Texture Analyser TA-XT2i (Stable Microsystems, United Kingdom) in compression mode was used to measure gel strength. The tests are conducted using a "force in compression" mode with a "return to start" test option. The force F (in N) required to compress the gel for a constant distance of 2.5 mm with an aluminium probe (1.0 cm in diameter) at a constant test speed (1.0 mm s^{-1}) was recorded as a compression function. Gels were also sectioned transversally and observed by SEM as described above. The experiments were repeated at least three times.

2.9. Statistical analysis

Statistical analysis was performed using R version 4.1.0 (2021-05-

18) and nlstools package (v1.0-2; Baty et al., 2015). Comparisons on the effect factors of treatment type and Power Intensity against response variables of particle size and gel strength were performed using generalised linear models (GLM). Post-hoc analysis was conducted using the Tukey test with confidence intervals and significance levels of $p < 0.05$ (*) and $p < 0.01$(**) were used. All measurements were made with 3 replicates. Pearson correlation was conducted between rheological model fits and experimental results.

3. Results and discussion

3.1. Polymer composition of mandarin pectin-rich polysaccharides (M-PRP)

Compositional analysis confirmed that M-PRP was composed primarily of pectin, with an uronic acid content of 44.7 ± 2.5%, neutral sugar content of 39.6 ± 2.3%, protein content of 6.8 ± 0.1% and ash 8.9 ± 0.1%. DM was 10.9 ± 1.2%.

We used a semi-quantitative technique based on ELISA to analyse the cell wall polymer composition of M-PRP (Rongkaumpan et al., 2019). We used 32 specific antibodies simultaneously to detect the soluble cell wall polymers present in the suspension, providing details of biopolymer composition. Seven polymers were most abundant in M-PRP, as shown in Table 2. Our results show that M-PRP contains an abundance of pectic polysaccharides, and the also presence of hemicellulose and extensin (a type of structural cell wall glycoprotein). Pectin epitopes detected order of abundance were un-esterified HG (epitopes LM19), RGI branched with linear galactan (epitopes LM5) and RGI branched with linear arabinan (epitopes LM6), methyl-esterified HG (epitopes LM20). This composition supports the chemical composition of acid and alkali extracted pectins from mandarin peel (Chen et al., 2021). Zhang et al. (2018b) showed that mandarin peel pectin consists mainly of RGI, with very high percentage of neutral sugar (79.7%). Dimopoulou et al. (2019) showed that lemon pectin is predominantly composed of HG (47–59%) with some arabinan-rich RGI (12–22%). These results suggest differences in the HG/RGI ratio between citrus tissues (e.g. peel versus membrane) and species (e.g. mandarin versus lemon). The cavitation treatments did not have significant effects on composition of M-PRP (data not shown).

3.2. Dispersibility of mandarin pectin-rich polysaccharides

Application of AC and HC for short times improved the dispersibility and stability of the M-PRP suspension compared to conventional stirring (Fig. 2). AC and HC treatments were significantly shorter (up to 180 s compared to 12 h stirring). The time refers to processing time, i.e. the time that the sample is under the experimental set up, and not the time that the sample is under cavitation conditions. For instance, the AC set up is static, the sample may be subjected to acoustic-generated power waves for most of the processing time, while the HC is a semi-continuous set up where there sample will only be subjected to cavitation during and immediately after the flow through the pump. The bulk of the sample will be in the holding tank. In the circulating HC system, comparable energy densities with the AC method may be achieved since repeated exposure to cavitation zone will occur, i.e. increased exposure frequency with increased processing time. This aspect is problematic to precisely determine given the static and dynamic experimental conditions but under the assumption that the sample experiences the repeated cavitation field then energy densities are equivalent. Considering these differences, AC and HC led to dispersions that remained stable up to 6 months (data not shown). The dispersion prepared by HC was particularly stable even after centrifugation (Fig. 2). HC treatment decreased the polydispersity index (PDI) by 13% from 0.78 to 0.68 compared to the control. However, suspensions prepared by AC (PDI 0.81) were not different in polydispersity compared with stirring (Fig. 2). All M-PRP suspensions can be considered as polydisperse (PDI >0.7) with a range of sized particles present in the dispersion. These particles are less polydisperse that obtained by AC by Ma et al. (2018).

Particle size results suggest that both HC and AC processing significantly reduced the size of suspended particles (Fig. 3). HC and AC for 180 s led to 51% and 30% smaller particles compared to stirred sample, though they were still relatively large (30–55 μm D[3,2]; 58–109 μm D[4,3]). The particle size (in both surface and volume) was constant under AC processing over time and with power intensity (Fig. 3). This is consistent with previous reports that observe little effect on particle size at intensities from 18 to 27 W mL^{-1} at 20 °C (Ma et al., 2018). Meanwhile, the trends in surface and volume properties were less clear under HC conditions. This could suggest deformation or partial aggregation of particles under some HC conditions leading to non-spherical particles.

The particles are likely to be molecular aggregates of pectin, hemicellulose and protein, suspended in the aqueous phase. According to the composition information, pectins (HG and branched RGI) are the most abundant component, followed by cellulose/hemicellulose fibrils and small amounts of glycoprotein. Pectins are known to decrease surface tension (Schmidt et al., 2015). Therefore, the more the particles disperse and the molecules solubilise, the more difficult it may be for the cavities for form.

SEM observation of the suspension (Fig. 4, abc) show the presence of fibre aggregates in stirred M-PRP, with a diameter of 10–90 nm (Fig. 4a arrow). The samples made by HC and AC processing for 150 s showed thicker fibre bundles of a diameter up to 280 nm (Fig. 4b arrow) and 520 nm (Fig. 4c, arrow) respectively. This suggest that the fibre bundle structures have been loosened, potentially through improved hydration and concomitant swelling of the biopolymers. These fibres are suggested to be cellulose-hemicellulose fibre bundles, which are co-extracted with pectins during segment solubilisation. Paximada et al. (2016) applied short AC treatment (20 kHz, up to 5 min, 25 °C) to bacterial cellulose and observed thickening and increased water-holding capacity of cellulose fibrils with treatments of 3 and 5 min. The AC treated suspensions had increased apparent viscosity and reduced phase separation over a 20 day storage time. Pinjari and Pandit (2010) used HC (cavitation number 2.61, flow rate 10.81 m/s, average pressure 7.8 kg/cm^2, for 6 h) to reduce the size of cellulose crystals from 63 to 1.3 μm, followed by a reduction to 300 nm using AC (22 kHz, 600 W, 1 h 50 min), accompanied by reduction in the degree of crystallinity of cellulose from 86.56% to 37.76%.

In order to observe the biopolymers at the nanoscale, AFM was used observe the M-PRP dispersions (Fig. 4, def). AFM micrographs showed typical of branched pectin molecules (Chen et al., 2021), though could also include the glycoproteins. These had a mean corrected diameter of 4.60 ± 0.06 nm (stirred), 5.42 ± 0.07 nm (AC), and 6.2 ± 0.1 nm (HC) respectively. The increase in diameter support the hypothesis that biopolymers are better hydrated with AC and HC treatment for 150 s compared to stirring for 12 h (Fig. 4, abc), without significant apparent degradation or debranching. This is in contrast to reports that AC treatment for 30 min (18.0–27 W mL^{-1}, 20 °C) was shown to reduce the molecular weight of pectin by 55% (Ma et al., 2018), increasing pectin's

Table 2
Cell wall composition of mandarin pectin-rich polysaccharides (M-PRP) measured using semi-quantitative ELISA. Data is mean of five replicate wells at A450 nm ± standard deviation, with stars representing relative strength of absorbance.

Class	Epitope	Antibody	Absorbance
Hemicellulose	Xyloglucan	LM25	0.62 ± 0.03*
Pectin	Un-esterified HG	LM19	1.70 ± 0.20***
	Esterified HG	LM20	0.78 ± 0.05*
	RGI galactan	LM5	1.88 ± 0.08***
	RGI arabinan	LM6-M	1.61 ± 0.08**
	RGI linear arabinan	LM13	0.31 ± 0.06
Protein	Extensin	JIM20	0.82 ± 0.12*

HG = homogalacturonan; RGI = rhamnogalacturonan.

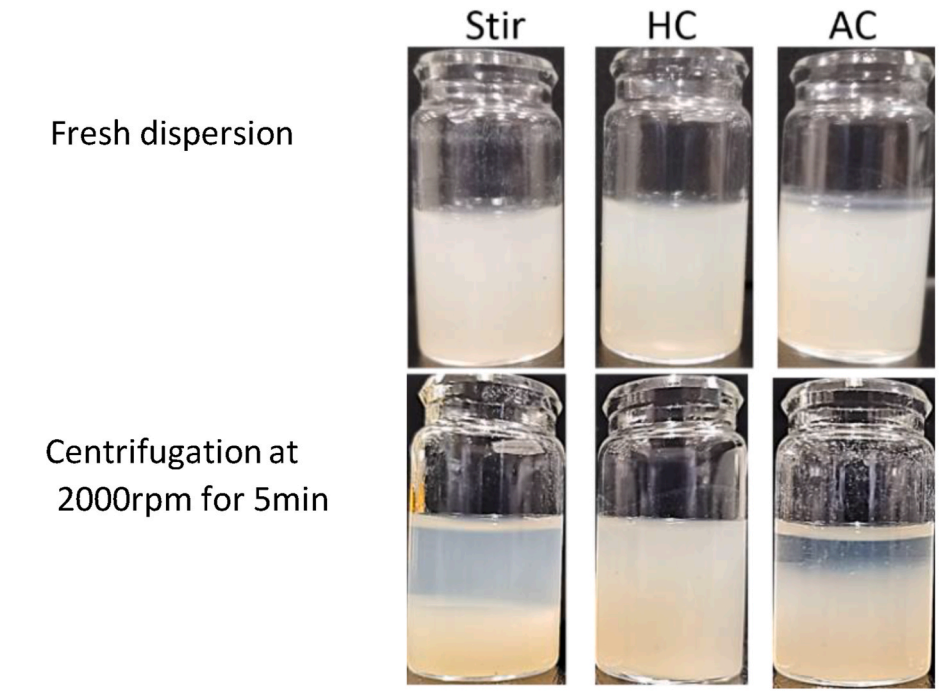

	Stir	HC	AC
Polydispersity index (PDI)	0.78±0.01[a]	0.68±0.00[b]	0.81±0.02[a]
Viscosity (Pa*s)	0.059±0.005[a]	0.30±0.005[b]	0.31±0.03[b]

Fig. 2. Mandarin pectin-rich polysaccharide (M-PRP) dispersions (1% in water) prepared by stirring for 12 h; hydrodynamic cavitation (HC) for 150 s; and acoustic cavitation (AC) for 150 s at room temperature. Table shows the polydispersity index (PDI) and apparent viscosity at a shear rate of 10^{-s} of the fresh dispersions. Data show mean of 3 replicate experiments with standard deviation. Different letters (a, b) indicate statistical difference between samples at a 95% confidence level.

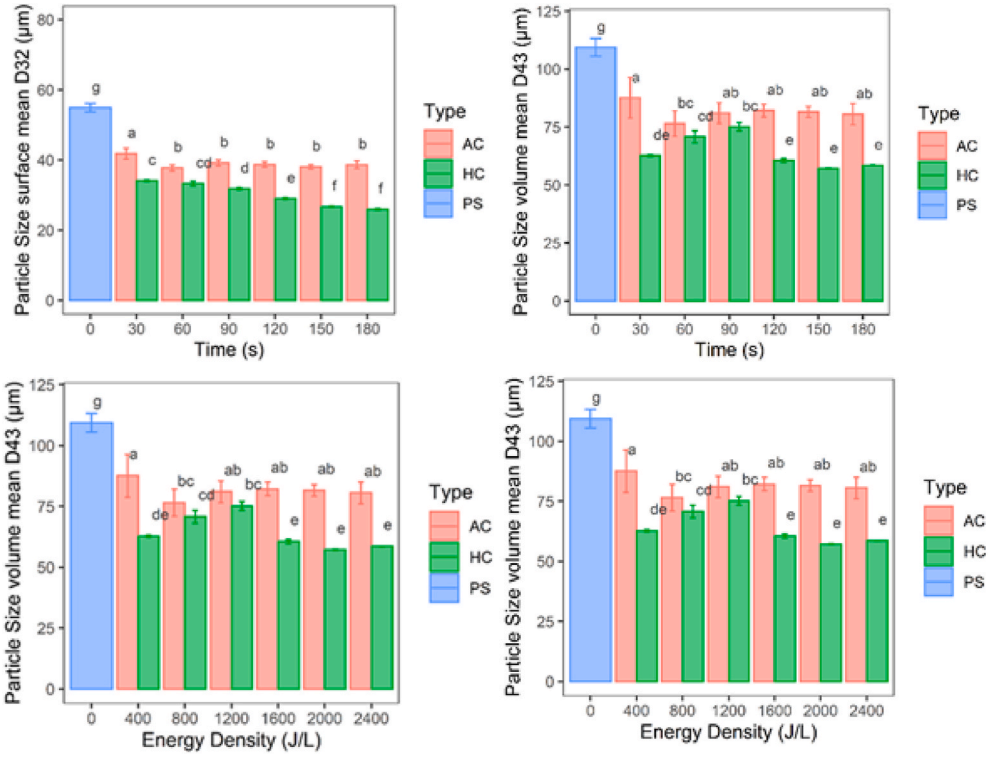

Fig. 3. Particle size (D[3,2] and D[4,3]) of mandarin pectin-rich polysaccharide (M-PRP) suspensions made using hydrodynamic cavitation (HC) and acoustic cavitation (AC) with a processing time for up to 180 s. Stirred sample (PS) was not cavitated (treatment time 0) but was stirred for 12 h. Bottom panels show the same data according to calculated energy density for cavitation methods. Data is mean of 5 replicate measurements with standard deviation. Different letters a, b, c indicate statistical difference between samples at a 95% confidence level.

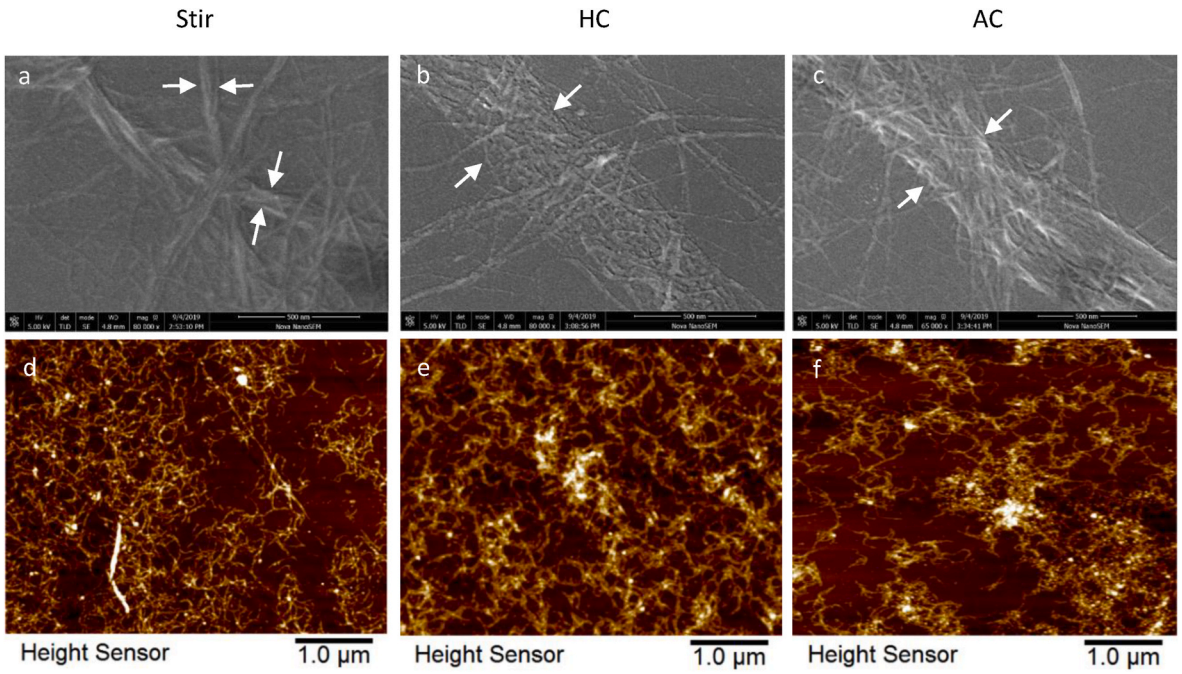

Fig. 4. Representative SEM and AFM images of 10 μg/ml M-PRP suspensions made by stirring for 12 h, hydrodynamic cavitation (HC) for 150 s; and acoustic cavitation (AC) for 150 s. a, b, c shows SEM observation under 80,000x magnification. d, e, f shows AFM observation.

susceptibility to enzymatic degradation. At the nano-scale, Tsai et al. (2008) observed 50% decrease in particle size following AC treatment of chitosan-sodium tripolyphosphate nanoparticles and suggested that the decrease in size of was due to fragmentation of the particle nanostructures, accompanied by chemical degradation of the chitosan polymers. The paper demonstrated that the size of the particles could be manipulated by varying different mechanical energy (leading to temperature rises) or mechanical shearing. The effects of heat and shear are hard to disentangle. Both are likely to have an effect even at the very short cavitation times used in the current study.

HC and AC treatments significantly increased the apparent viscosity of the pectin suspensions across all shear rates evaluated (Fig. 5). This is attributed to improved dispersion of large particles, combined with hydration and potentially increased entanglement between biopolymers. Power Law fits show good fit and Pearson correlations between log transformed data of shear rate and log viscosities of stirred pectin (PS, r = −0.84), AC (r = −0.77), HC (r = −0. 82). All treatment types have $n < 1$ indicating shear thinning behaviour and apparent viscosities are such that AC > HC > PS. Significant differences $p < 0.001$ in viscosity at 10 s^{-1} between stirred (PS) and both HC and AC but no difference between AC and HC.

Other studies have shown a decrease in viscosity of pectin suspensions following much longer AC treatments (12.56 W/cm^2, 30 min) attributed to degradation of polymers (Wang et al., 2015). The breakdown of macromolecules was explained by chemical effects of reactive species or physical effects of high pressure jets formed during cavity

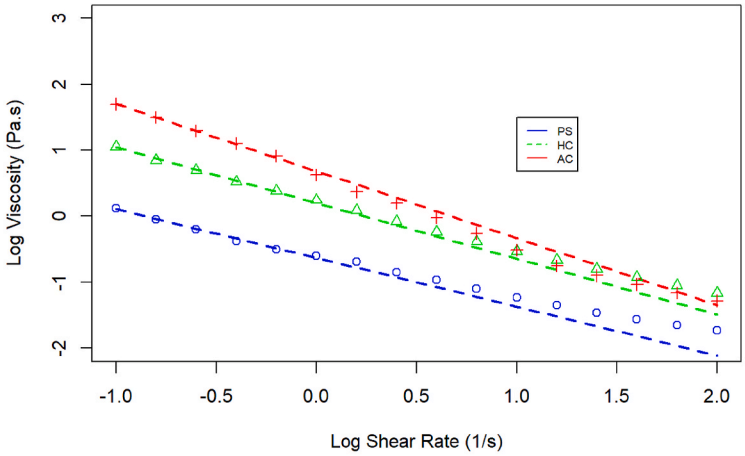

Pectin

	Estimate	Std. Error	t value	Pr(>|t|)
K	0.2334	0.0092	25.3372	0
n	0.2607	0.0203	12.8599	0

HC

	Estimate	Std. Error	t value	Pr(>|t|)
	1.5772	0.0594	26.5403	0
	0.1561	0.0189	8.2695	0

AC

	Estimate	Std. Error	t value	Pr(>|t|)
	4.8339	0.1021	47.3441	0.0000
	-0.0163	0.0102	-1.5879	0.1346

Fig. 5. Apparent viscosity of M-PRP pectin suspension prepared by stirring for 12 h (PS), acoustic cavitation for 150 s (AC) and hydrodynamic cavitation for 150 s (HC) and parameter estimates (K, n) for each method. Data points show average of 3 replicate experiments.

collapse. There is likely to be a threshold, as yet to be determined, at which the particles and biopolymers will start to breakdown significantly to decrease the viscosity.

3.3. Gelling properties

M-PRP has low level of esterification (10.9%) due to the process of alkaline extraction, which removes methyl esters in a random fashion. The low DM pectin is expected to show good gelling property upon adding calcium (Willats et al., 2001; Chen et al., 2021).

Fig. 6 shows the mechanical strength of M-PRP-calcium gels under compression forces. Gels made by AC and HC were significantly stronger (4 fold and 7 fold respectively at 150 s) than those prepared with stirred M-PRP. Gels made with AC showed higher strength than HC for most time points except 150 and 180 s. Improved dispersion and hydration can explain increases gel strength by increasing opportunities for intermolecular bonding. The gels made with AC had good strength, which remained the same over treatment time. This observation suggests rapid dispersion the polymers occurred in very short time, supporting earlier particle size and viscosity observations. Under HC treatment, gel strength was only significantly stronger after 150 s of treatment, suggesting dispersion is less rapid by HC compared to AC. But after 150 s, HC showed significant higher strength than AC (Fig. 6). The differences may be attributed to the close nature of the AC system, where molecules would be subjected to cavitation effects for the duration of the treatment. Meanwhile, in HC, a fraction of the dispersion is pumped through the cavitation unit, while the rest is in the holding tank. Even considering this difference, the treatment times are much shorter than have been reported previously.

Cheng et al. (2019) showed that the hardness of emulsion protein gels increased with increasing AC time (5 min–20 min). However, even longer AC treatment (30 min–60 min) and higher intensity (up to 40 W/cm^2) were associated with decreased gel strength, again attributed to an overall reduction of average molecular weight of pectin (Seshadri et al., 2003). M-PRP is rich in RGI especially in arabinose, which might potentially contribute to the gelling properties. Zheng et al. (2020) studied the role of arabinose-rich RGI side-chains in cation gelation of mandarin pectin. They showed that enzymatically-debranched pectin formed gels that were at least 50% weaker compared to gels made with the original pectin (Zheng et al., 2020). The better hydration of the M-PRP RGI side chains, as suggested by the AFM images, as well as its balanced composition of de-methylated HG and branched RGI could contribute to strong gelling performance.

Fig. 7 shows observations of transverse sections of the M-PRP gels. Gels were freeze-dried first to preserve their structure for SEM observation. Gels made with stirred M-PRP show heterogeneous porous structures (Fig. 7, d), with visible pores with sizes ranging from 75 μm to 300 μm (Fig. 7, d arrows). Gels made with M-PRP dispersed by HC (Fig. 7, e) and AC (Fig. 7, f) for 150 s show more homogeneous structure with smooth surfaces and no apparent pores (Fig. 7h and i). The presence of large pores in gels made by stirring explain their weaker mechanical strength. Similar to our stirred sample (Fig. 7, g), similar porous structures have been observed in calcium-pectin gels (Sriamornsak, 1999; Sriamornsak et al., 2008; Sriamornsak and Nunthanid, 1999; Guo et al., 2014; Chen et al., 2021). Sriamornsak et al. (2008) claimed that the homogeneous diffusion of calcium into the polymer network is important to make mechanically stronger gels. Improved dispersion of polymers in AC and HC samples would possibly improve diffusion of calcium, explaining the stronger gels observed. AC (20 kHz, 100 W ml^{-1}, 30 min, max 50 °C) has also been used to make high DM (64–70%) pectin-sugar gels. The effects on the rheological properties of the gels varied by dispersion method (overhead stirrer, magnetic stirrer and stirring combined with AC) and pectin type (Muñoz-Labrador et al., 2018).

4. Conclusion and prospects

Many studies have investigated the effects of AC on pectin extraction and molecular properties (e.g. molecular size). We are the first study to compare AC and HC treatments, focusing on very short treatment times (up to 180 s). The key findings were that short-time AC and HC treatments were effective at forming stable dispersions of low-methoxy pectin without observable changes to polymer composition. HC and AC processing significantly reduced the size of suspended particles by 51% and 30% respectively, with AC following a more predictable decrease over time compared to HC. HC and AC treatments significantly increased the apparent viscosity of the pectin suspensions across all shear rates evaluated. All treatment types have $n < 1$ indicating shear thinning behaviour and apparent viscosities are such that AC > HC > stirred pectin. The microscopic observations suggest these short cavitation treatments improve hydration of the fibres and matrix polysaccharides present in the suspensions.

It is difficult to compare the experimental set ups, as the AC used here is a static set up where the bulk of the suspension will be subjected to the power waves, while in the semi-dynamic HC set up, only a fraction of the suspension will be subjected to cavitation at any one time. With such short experiments, it may be difficult to differentiate between cavitation and bulk flow effects. Combining AC and HC with microfluidic imaging would allow a better understanding of cavity formation in pectin solutions/dispersions. However, the results show similar improvements (with subtle differences) in the stability of the suspensions and the gelling properties. These are explained by improved dispersion and hydration of the biomolecules present, primarily pectins. The theory behind cavitation suggests that bubble collapse near the surface of the

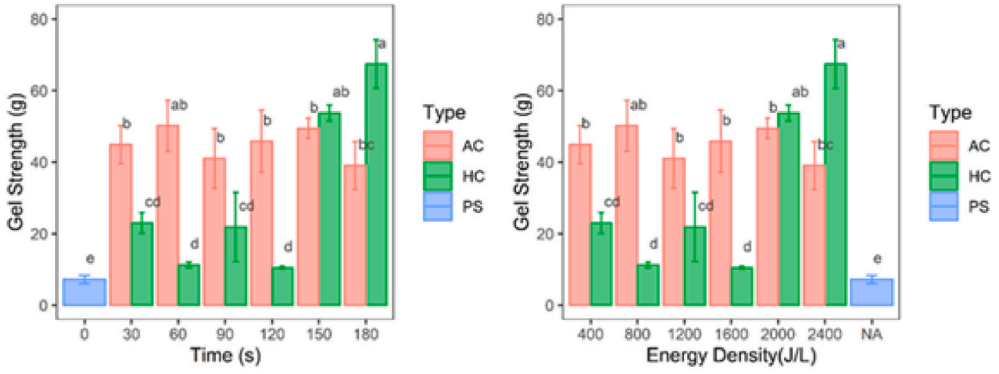

Fig. 6. Gel strength (compression yield point) prepared under different treatments. Gels were made by adding calcium (35 mM) into M-PRP suspension which was made by stirring for 12 h (PS), hydrodynamic cavitation (HC) and acoustic cavitation (AC) for up to 180 s. Data show mean of 3 replicate experiments with standard deviation. Different letters a, b, c indicate statistical difference between samples at a 95% confidence level.

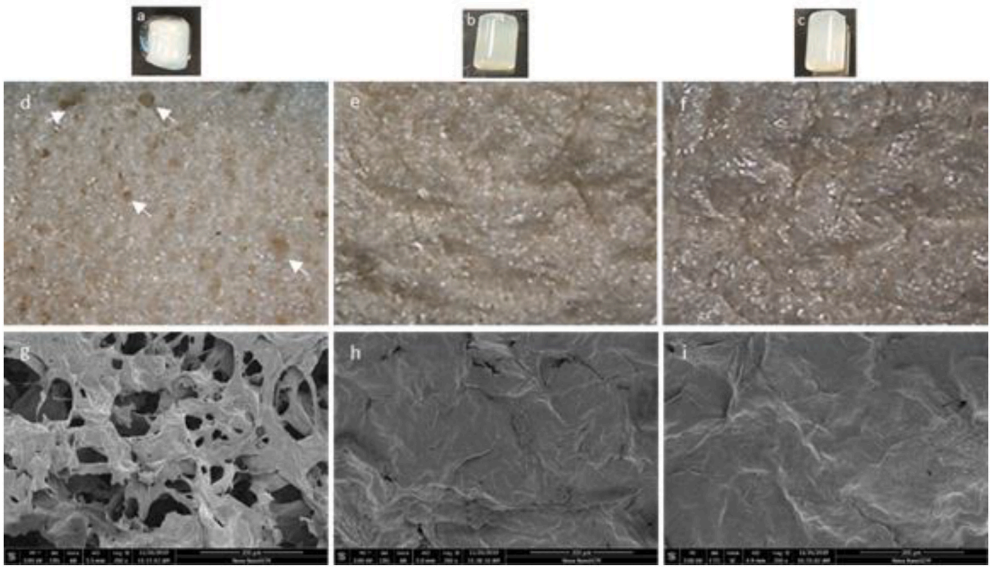

Fig. 7. Representative images of calcium gel structure (gels were made from M-PRP suspension made by stirring for 12 h, hydrodynamic cavitation (HC, 150 s) and acoustic cavitation (AC, 150 s) treatment, with addition of 35 mM CaCl2). a,b,c shows gel beads; d,e,f shows gel cross-section structure after freeze-drying; g,h,i shows SEM microscope under 200x magnification.

particles may cause an asymmetric liquid jet that, combined with shear and thermal effects, can reduce the size of particles. Furthermore, the generation of reactive species can chemically fragment molecules.

In contrast to many studies, we did not observed changes to pectin composition or fragmentation. Longer cavitation methods have been shown to reduce the molecular weight and DM of pectin (Ma et al., 2018), but eventually may lead to particle aggregation (Zhang et al., 2013) and clouding (Sattar et al., 2019). The optimal conditions for dispersion need to be optimised depending on the nature of the pectin, as dispersing treatments have different effects depending on pectin composition (Muñoz-Labrador et al., 2018). The generation of reactive species in the short-scale process needs further investigation.

At the molecular level, we did not observe fragmented or debranched biopolymers when observed under SEM or AFM. However, better characterisation of the samples molecular weight and size by chromatography is needed to confirm this. More likely cavitation contributed to the rapid hydration and swelling of the biopolymers, as has been observed for bacterial cellulose under short AC treatments (Paximada et al., 2016). The effect of solvent and other solutes could have important implications. As noted earlier, as pectin dissolves and decreases the surface tension of water, reducing cavity formation and stability.

The possibility to combine AC and HC with enzymatic modification of biopolymers (carbohydrates or proteins) offers exiting opportunities to modulate their rheological properties for relevant applications (Ma et al., 2018). Further research should also investigate the effect of AC and HC on gel properties, with the aim to fine-tune pore size, using not only calcium but also heat and acid/sugar gels (Muñoz-Labrador et al., 2018). Investigation of gel deformation, stability and melting properties of these pectin-calcium gels are needed. Furthermore, the porosity of the gels needs exploring for potential bioactive release applications.

For food industrial applications where stable dispersibility and stability is required (e.g. fruit juice, plant milk alternatives), short-time cavitation treatments seem promising dispersing methods for cleaner production. Further research should focus on industrial-relevant scales, in batch or semi-continuous set ups, with consideration of energy utilisation and conservation.

Funding

This work was supported by Innovate UK, the BBSRC (grant number BB/S020950/1) and National Key Research and Development program of China (grant number 2017YFE0122300), under the Newton Fund Scheme. HL was funded by an EPSRC-SOFI CDT Ph.D. studentship supported by PepsiCo Inc. "The views and opinions expressed in this presentation are those of the author and do not necessarily reflect the position or policy of PepsiCo Inc."

CRediT authorship contribution statement

Jin Chu: Conceptualization, Formal analysis, Investigation, Writing – original draft. **Philip Metcalfe:** Conceptualization, Methodology, Formal analysis. **Holly V. Linford:** Investigation, Formal analysis. **Siying Zhao:** Investigation, Formal analysis. **Francisco M. Goycoolea:** Conceptualization. **Shiguo Chen:** Conceptualization, Funding acquisition. **Xingqian Ye:** Conceptualization, Funding acquisition. **Melvin Holmes:** Formal analysis, writing. **Caroline Orfila:** Funding acquisition, Conceptualization, Writing – original draft, Writing – review & editing, Project administration, Supervision.

Declaration of competing interest

Philip Metcalfe is founder and CEO of Biopower Ltd. The authors declare no conflicts of interest.

Acknowledgements

Our special thanks to Xiangshan Huayu Foodstuffs Co. Ltd for providing the M-PRP and Neil Rigby for technical assistance with rheological measurements.

Appendix A. Supplementary data

Supplementary data to this article can be found online at https://doi.org/10.1016/j.jclepro.2021.129789.

References

Alba, K., Kontogiorgos, V., 2017. Pectin at the oil-water interface: relationship of molecular composition and structure to functionality. Food Hydrocolloids 68, 211–218.

Albanese, L., Ciriminna, R., Meneguzzo, F., Pagliaro, M., 2015. Energy efficient inactivation of Saccharomyces cerevisiae via controlled hydrodynamic cavitation. Energy Science & Engineering 3, 221–238.
Albanese, L., Ciriminna, R., Meneguzzo, F., Pagliaro, M., 2017. Beer-brewing powered by controlled hydrodynamic cavitation: theory and real-scale experiments. J. Clean. Prod. 142, 1457–1470.
Ashokkumar, M., 2015. Applications of ultrasound in food and bioprocessing. Ultrason. Sonochem. 25, 17–23.
Ashokkumar, M., Rink, R., Shestakov, S., 2011. Hydrodynamic Cavitation – an Alternative to Ultrasonic Food Processing. Technical Acoustics, pp. 1–10.
Baty, F, Ritz, C, Charles, S, Brutsche, M, Flandrois, J.P., Delignette-Muller, M.L., 2015. A Toolbox for Nonlinear Regression in R: The Package nlstools. J. Stat. Software 66 (5), 1–21. https://doi.org/10.18637/jss.v066.i05.
Cesaretti, M., Luppi, E., Maccari, F., Volpi, N., 2003. A 96-well assay for uronic acid carbazole reaction. Carbohydr. Polym. 54, 59–61.
Chan, S.Y., Choo, W.S., Young, D.J., Loh, X.J., 2017. Pectin as a rheology modifier: origin, structure, commercial production and rheology. Carbohydr. Polym. 161, 118–139.
Chen, J., Cheng, H., Wu, D., Linhardt, R.J., Zhi, Z., Yan, L., Chen, S., Ye, X., 2017. Green recovery of pectic polysaccharides from citrus canning processing water. J. Clean. Prod. 144, 459–469.
Chen, S., Zheng, J., Zhang, L., Cheng, H., Orfila, C., Ye, X., Chen, J., 2021. Synergistic gelling mechanism of RG-I rich citrus pectic polysaccharide at different esterification degree in calcium-induced gelation. Food Chem. 350, 129177.
Cheng, Y., Donkor, P.O., Ren, X., Wu, J., Agyemang, K., Ayim, I., Ma, H., 2019. Effect of ultrasound pretreatment with mono-frequency and simultaneous dual frequency on the mechanical properties and microstructure of whey protein emulsion gels. Food Hydrocolloids 89, 434–442.
Chu, J., Ho, P., Orfila, C., 2020. Growth region impacts cell wall properties and hard-to-cook phenotype of canned navy beans (Phaseolus vulgaris). Food Bioprocess Technol. 13, 818–826.
Chu, J., Igbetar, B.D., Orfila, C., 2017. Fibrous cellular structures are found in a commercial fruit smoothie and remain intact during simulated digestion. J. Nutr. Food Sci. 7, 576.
Coll-Almela, L., Saura-López, D., Laencina-Sánchez, J., Schols, H.A., Voragen, A.G.J., Ros-García, J.M., 2015. Characterisation of cell-wall polysaccharides from Mandarin segment membranes. Food Chem. 175, 36–42.
Cui, J., Ren, W., Zhao, C., Gao, W., Tian, G., Bao, Y., Lian, Y., Zheng, J., 2019. The Structure–Property Relationships of Acid- and Alkali-Extracted Grapefruit Peel Pectins. Carbohydrate Polymers, p. 115524.
Dimopoulou, M., Alba, K., Campbell, G., Kontogiorgos, V., 2019. Pectin recovery and characterization from lemon juice waste streams. J. Sci. Food Agric. 99, 6191–6198.
FAO, 2016. In: Markets and Trade Division, RAMHOT products team (Ed.), Citrus Fruit Fresh and Processed, Statistical Bulletin. FAO (ROME).
Ghorbani, M., Olofsson, K., Benjamins, J.-W., Loskutova, K., Paulraj, T., Wiklund, M., Grishenkov, D., Svagan, A.J., 2019. Unravelling the acoustic and thermal responses of perfluorocarbon liquid droplets stabilized with cellulose nanofibers. Langmuir 35, 13090–13099.
Gogate, P.R., 2011. Hydrodynamic cavitation for food and water processing. Food Bioprocess Technol. 4, 996–1011.
Guo, X., Duan, H., Wang, C., Huang, X., 2014. Characteristics of two calcium pectinates prepared from citrus pectin using either calcium chloride or calcium hydroxide. J. Agric. Food Chem. 62, 6354–6361.
INGREDION, 2014. The Clean Label Guide to Europe.
Katariya, P., Arya, S.S., Pandit, A.B., 2020. Novel, non-thermal hydrodynamic cavitation of orange juice: effects on physical properties and stability of bioactive compounds. Innovat. Food Sci. Emerg. Technol. 62, 102364.
Kpodo, F.M., Agbenorhevi, J.K., Alba, K., Oduro, I.N., Morris, G.A., Kontogiorgos, V., 2018. Structure-function relationships in pectin emulsification. Food Biophys. 13, 71–79.
Ma, X., Wang, D., Chen, W., Ismail, B.B., Wang, W., Lv, R., Ding, T., Ye, X., Liu, D., 2018. Effects of ultrasound pretreatment on the enzymolysis of pectin: kinetic study, structural characteristics and anti-cancer activity of the hydrolysates. Food Hydrocolloids 79, 90–99.
Mamma, D., Christakopoulos, P.J.W., Valorization, B., 2014. Biotransformation of citrus by-products into value added products. Waste and Biomass Valorization 5, 529–549.
Mao, G., Wu, D., Wei, C., Tao, W., Ye, X., Linhardt, R.J., Orfila, C., Chen, S., 2019. Reconsidering conventional and innovative methods for pectin extraction from fruit and vegetable waste: targeting rhamnogalacturonan I. Trends Food Sci. Technol. 94, 65–78.
Meneguzzo, F., Brunetti, C., Fidalgo, A., Ciriminna, R., Delisi, R., Albanese, L., Zabini, F., Gori, A., Dos Santos Nascimento, L.B., De Carlo, A., Ferrini, F., Ilharco, L.M., Pagliaro, M., 2019. Real-scale integral valorization of waste orange peel via hydrodynamic cavitation, 7, 581.
Milly, P.J., Toledo, R.T., Harrison, M.A., Armstead, D., 2007. Inactivation of food spoilage microorganisms by hydrodynamic cavitation to achieve pasteurization and sterilization of fluid foods. J. Food Sci. 72, M414–M422.
Milly, P.J., Toledo, R.T., Kerr, W.L., Armstead, D., 2008. Hydrodynamic cavitation: characterization of a novel design with energy considerations for the inactivation of Saccharomyces cerevisiae in apple juice. J. Food Sci. 73, M298–M303.
Morris, G.A., Foster, T.J., Harding, S.E., 2000. The effect of the degree of esterification on the hydrodynamic properties of citrus pectin. Food Hydrocolloids 14, 227–235.
Morris, V.J., Gunning, A.P., Kirby, A.R., Round, A., Waldron, K., Ng, A., 1997. Atomic force microscopy of plant cell walls, plant cell wall polysaccharides and gels. Int. J. Biol. Macromol. 21, 61–66.
Muñoz-Labrador, A., Moreno, R., Villamiel, M., Montilla, A., 2018. Preparation of citrus pectin gels by power ultrasound and its application as an edible coating in strawberries. J. Sci. Food Agric. 98, 4866–4875.
Pattathil, S., Avci, U., Baldwin, D., Swennes, A.G., Mcgill, J.A., Popper, Z., Bootten, T., Albert, A., Davis, R.H., Chennareddy, C., Dong, R., O'shea, B., Rossi, R., Leoff, C., Freshour, G., Narra, R., O'neil, M., York, W.S., Hahn, M.G., 2010. A comprehensive toolkit of plant cell wall glycan-directed monoclonal antibodies, 153, 514–525.
Paximada, P., Dimitrakopoulou, E.A., Tsouko, E., Koutinas, A.A., Fasseas, C., Mandala, I. G., 2016. Structural modification of bacterial cellulose fibrils under ultrasonic irradiation. Carbohydr. Polym. 150, 5–12.
Perrin, L., Colombet, D., Ayela, F., 2021. Comparative study of luminescence and chemiluminescence in hydrodynamic cavitating flows and quantitative determination of hydroxyl radicals production. Ultrason. Sonochem. 70, 105277.
Pinjari, D.V., Pandit, A.B., 2010. Cavitation milling of natural cellulose to nanofibrils. Ultrason. Sonochem. 17, 845–852.
Rabiti, D., Orfila, C., Holmes, M., Bordoni, A., Sarkar, A., 2018. In vitro oral processing of raw tomato: novel insights into the role of endogenous fruit enzymes. J. Texture Stud. 49, 351–358.
Rongkaumpan, G., Amsbury, S., Andablo-Reyes, E., Linford, H., Connell, S., Knox, J.P., Sarkar, A., Benitez-Alfonso, Y., Orfila, C., 2019. Cell wall polymer composition and spatial distribution in ripe banana and mango fruit: implications for cell adhesion and texture perception. Front. Plant Sci. 10.
Sattar, S., Imran, M., Mushtaq, Z., Ahmad, M.H., Holmes, M., Maycock, J., Khan, M.I., Yasmin, A., Khan, M.K., Muhammad, N., 2019. Functional quality of optimized peach-based beverage developed by application of ultrasonic processing. Food Sci. Nutr. 7, 3692–3699.
Save, S.S., Pandit, A.B., Joshi, J.B., 1997. Use of hydrodynamic cavitation for large scale microbial cell disruption. Food Bioprod. Process. 75, 41–49.
Schmidt, U.S., Schmidt, K., Kurz, T., Endreß, H.U., Schuchmann, H.P., 2015. Pectins of different origin and their performance in forming and stabilizing oil-in-water-emulsions. Food Hydrocolloids 46, 59–66.
Seshadri, R., Weiss, J., Hulbert, G.J., Mount, J., 2003. Ultrasonic processing influences rheological and optical properties of high-methoxyl pectin dispersions. Food Hydrocolloids 17, 191–197.
Sharma, K., Mahato, N., Cho, M.H., Lee, Y.R., 2017. Converting citrus wastes into value-added products: economic and environmentally friendly approaches. Nutrition 34, 29–46.
Sivakumar, M., Pandit, A.B., 2002. Wastewater treatment: a novel energy efficient hydrodynamic cavitational technique. Ultrason. Sonochem. 9, 123–131.
Sriamornsak, P., 1999. Effect of calcium concentration, hardening agent and drying condition on release characteristics of oral proteins from calcium pectinate gel beads. Eur. J. Pharmaceut. Sci. 8, 221–227.
Sriamornsak, P., Nunthanid, J., 1999. Calcium pectinate gel beads for controlled release drug delivery: II. Effect of formulation and processing variables on drug release. J. Microencapsul. 16, 303–313.
Sriamornsak, P., Thirawong, N., Cheewatanakornkool, K., Burapapadh, K., Sae-Ngow, W., 2008. Cryo-scanning electron microscopy (cryo-SEM) as a tool for studying the ultrastructure during bead formation by ionotropic gelation of calcium pectinate. Int. J. Pharm. 352, 115–122.
Sun, X., Liu, J., Ji, L., Wang, G., Zhao, S., Yoon, J.Y., Chen, S., 2020. A review on hydrodynamic cavitation disinfection: the current state of knowledge. Sci. Total Environ. 737, 139606.
Taboada, E., Fisher, P., Jara, R., Zúñiga, E., Gidekel, M., Cabrera, J.C., Pereira, E., Gutiérrez-Moraga, A., Villalonga, R., Cabrera, G., 2010. Isolation and characterisation of pectic substances from murta (Ugni molinae Turcz) fruits. Food Chem. 123, 669–678.
Tsai, M.L., Bai, S.W., Chen, R.H., 2008. Cavitation effects versus stretch effects resulted in different size and polydispersity of ionotropic gelation chitosan–sodium tripolyphosphate nanoparticle. Carbohydr. Polym. 71, 448–457.
Varela, P., Fiszman, S.M., 2013. Exploring consumers' knowledge and perceptions of hydrocolloids used as food additives and ingredients. Food Hydrocolloids 30, 477–484.
Voragen, A.G.J., Coenen, G.J., Verhoef, R.P., Schols, H.A., 2009. Pectin, a versatile polysaccharide present in plant cell walls. Struct. Chem. 20, 263–275.
Voragen, A.G.J., Pilnik, W., Thibault, J.F., Axelos, M.A.V., Renard, C.M.G.C., 1995. Pectins. In: STEPHAN, A.M. (Ed.), Food Polysaccharides and Their Applications. Marcel Dekker, New York.
Wang, W., Chen, W., Zou, M., Lv, R., Wang, D., Hou, F., Feng, H., Ma, X., Zhong, J., Ding, T., Ye, X., Liu, D., 2018. Applications of power ultrasound in oriented modification and degradation of pectin: a review. J. Food Eng. 234, 98–107.
Wang, W., Ma, X., Xu, Y., Cao, Y., Jiang, Z., Ding, T., Ye, X., Liu, D., 2015. Ultrasound-assisted heating extraction of pectin from grapefruit peel: optimization and comparison with the conventional method. Food Chem. 178, 106–114.
Willats, W.G.T., Orfila, C., Limberg, G., Buchholt, H.C., Van Alebeek, G.J.W.M., Voragen, A.G.J., Marcus, S.E., Christensen, T.M.I.E., Mikkelsen, J.D., Murray, B.S., Knox, J.P., 2001. Modulation of the degree and pattern of methyl-esterification of pectic homogalacturonan in plant cell walls - implications for pectin methyl esterase action, matrix properties, and cell adhesion. J. Biol. Chem. 276, 19404–19413.
Williams, B.A., Mikkelsen, D., Flanagan, B.M., Gidley, M.J., 2019. "Dietary fibre": moving beyond the "soluble/insoluble" classification for monogastric nutrition, with an emphasis on humans and pigs. J. Anim. Sci. Biotechnol. 10, 45.
Yan, L., Ye, X., Linhardt, R.J., Chen, J., Yu, D., Huang, R., Liu, D., Chen, S., 2018. Full recovery of value-added compounds from citrus canning processing water. J. Clean. Prod. 176, 959–965.
Zema, D.A., Calabrò, P.S., Folino, A., Tamburino, V., Zappia, G., Zimbone, S.M., 2018. Valorisation of citrus processing waste: a review. Waste Manag. 80, 252–273.

Zhang, H., Chen, J., Li, J., Wei, C., Ye, X., Shi, J., Chen, S., 2018a. Pectin from citrus canning wastewater as potential fat replacer in ice cream. Molecules 23, 925.
Zhang, H., Chen, J., Li, J., Yan, L., Li, S., Ye, X., Liu, D., Ding, T., Linhardt, R.J., Orfila, C., Chen, S., 2018b. Extraction and characterization of RG-I enriched pectic polysaccharides from Mandarin citrus peel. Food Hydrocolloids 79, 579–586.
Zhang, L.F., Ye, X.Q., Xue, S.J., Zhang, X.Z., Liu, D.H., Meng, R.F., Chen, S.G., 2013. Effect of high-intensity ultrasound on the physicochemical properties and nanostructure of citrus pectin. J. Sci. Food Agric. 93, 2028–2036.
Zheng, J., Chen, J., Zhang, H., Wu, D., Ye, X., Linardt, R.J., Chen, S., 2020. Gelling mechanism of RG-I enriched citrus pectin: role of arabinose side-chains in cation- and acid-induced gelation. Food Hydrocolloids 101, 105536.
Zupanc, M., Pandur, Ž., Stepišnik Perdih, T., Stopar, D., Petkovšek, M., Dular, M., 2019. Effects of cavitation on different microorganisms: the current understanding of the mechanisms taking place behind the phenomenon. A review and proposals for further research. Ultrason. Sonochem. 57, 147–165.